Potentiometric Determination of the Gibbs Energies of Formation of $SrZrO_3$ and $BaZrO_3$

K.T. JACOB and Y. WASEDA

The Gibbs free energies of formation of strontium and barium zirconates have been determined in the temperature range 960 to 1210 K using electrochemical cells incorporating the respective alkaline-earth fluoride single crystals as solid electrolytes. Pure strontium and barium monoxides were used in the reference electrodes. During measurements on barium zirconate, the oxygen partial pressure in the gas phase over the electrodes was maintained at a low value of 18.7 Pa to minimize the solubility of barium peroxide in the monoxide phase. Strontium zirconate was found to undergo a phase transition from orthorhombic perovskite (o) with space group *Cmcm*; D_{2h}^{17} to tetragonal perovskite (t) having the space group $14/mcm$; D_{4h}^{18} at 1123 (± 10) K. Barium zirconate does not appear to undergo a phase transition in the temperature range of measurement. It has the cubic perovskite (c) structure. The standard free energies of formation of the zirconates from their component binary oxides AO (A = Sr, Ba) with rock salt (rs) and ZrO_2 with monoclinic (m) structures can be expressed by the following relations:

$$SrO\ (rs) + ZrO_2\ (m) \rightarrow SrZrO_3\ (o)$$

$$\Delta G^\circ = -74{,}880 - 14.2T\ (\pm 200)\ J\ mol^{-1}$$

$$SrO\ (rs) + ZrO_2\ (m) \rightarrow SrZrO_3\ (t)$$

$$\Delta G^\circ = -73{,}645 - 15.3T\ (\pm 200)\ J\ mol^{-1}$$

$$BaO\ (rs) + ZrO_2\ (m) \rightarrow BaZrO_4\ (c)$$

$$\Delta G^\circ = -127{,}760 - 1.79T\ (\pm 250)\ J\ mol^{-1}$$

The results of this study are in reasonable agreement with calorimetric measurements reported in the literature. Systematic trends in the stability of alkaline-earth zirconates having the stoichiometry $AZrO_3$ are discussed.

I. INTRODUCTION

THERE is current interest in oxides with perovskite structure that exhibit ionic conduction.[1] Recent electrochemical measurements by the authors indicate that both pure and doped $SrZrO_3$ and $SrHfO_3$ are good oxide-ion conductors that can be used as sensors for oxygen in liquid metals. Because of the new prominence of alkaline-earth zirconates and hafnates as solid electrolytes, systematic studies have been conducted on their free energies of formation. This article reports measurements on $SrZrO_3$ and $BaZrO_3$. A study on $CaZrO_3$ is published elsewhere.[2] The thermodynamic information is useful for assessing potential interactions of these materials with liquid metals, support materials, and auxiliary electrodes.

Both strontium and barium zirconates are formed in the fuel pins of nuclear reactors under normal operating conditions of temperature and oxygen chemical potential.[3] The fission products, strontium and zirconium, react with oxygen in $UO_{2\pm\delta}$ or $(U, Pu)O_{2\pm\delta}$ fuel to form the zirconate. They are also formed by the reaction of strontium and barium with oxidized ZIRCALOY* cladding.[4] High-temperature thermodynamic properties of the compounds are therefore needed for the evaluation of fuel-fission product interactions and are relevant to nuclear technology.

*ZIRCALOY is a trademark of Westinghouse Electric Company, Pittsburgh, PA.

The low-temperature heat capacities of $SrZrO_3$ and $BaZrO_3$ have been measured in the temperature range 51 to 296 K by King and Weller.[5] The standard entropies calculated from the measurements are as follows:

$$S^\circ_{298.15K}\ (SrZrO_3) = 115.0\ (\pm 2)\ J\ K^{-1}\ mol^{-1}$$

$$S^\circ_{298.15K}\ (BaZrO_3) = 124.7\ (\pm 2)\ J\ K^{-1}\ mol^{-1}$$

Levitskii *et al.*[6] have measured high-temperature enthalpy increments of $SrZrO_3$ and $BaZrO_3$ from 300 to 1650 K by drop calorimetry. Nagarajan *et al.*[7] have reported enthalpy increments for $SrZrO_3$ and $BaZrO_3$ from 1030 to 1687 K, using high-temperature differential calorimetry. Drop calorimetry has been used by Fomichev *et al.*[8] for measurements on $SrZrO_3$ from 526 to 2318 K and by Cordfunke and Konings[9] on $BaZrO_3$ from 407 to 775 K. L'vova and Fedos'ev[10] have determined the enthalpies of reaction of ACO_3 (A = Sr, Ba) and ZrO_2 in a bomb calorimeter, carbon black being used as the

K.T. JACOB, Chairman and Professor, Materials Research Center, and Professor, Department of Metallurgy, is with Indian Institute of Science, Bangalore 560012, India. Y. WASEDA, Director, Institute for Advanced Materials Processing, is with Tohoku University, Sendai 980, Japan.

Manuscript submitted August 1, 1994.

initiating substance. Corrections were applied for incomplete reaction and combustion of carbon black. From the enthalpy changes for reactions of the type

$$ACO_3\,(s) + ZrO_2\,(s) \rightarrow AZrO_3\,(s) + CO_2\,(g) \quad [1]$$

the enthalpies of formation of $AZrO_3$ (A = Sr, Ca) can be calculated using auxiliary data for ACO_3 and CO_2 from the literature. More recently, Muromachi and Navrotsky[11] have determined the enthalpies of solution of $SrZrO_3$ and $BaZrO_3$ in molten $LiBO_2$-$NaBO_2$ at 1060 K. By combining these values with enthalpies of solution of SrO, BaO, and ZrO_2, determined separately under the same conditions, they obtained the enthalpies of formation of $AZrO_3$ (A = Sr, Ba) from their component binary oxides.

The standard free energy of formation of $SrZrO_3$ from its component oxides was measured directly by Levitskii[12] using the solid-state cell

$$Pt, O_2, SrO + SrF_2|CaF_2|SrZrO_3 + ZrO_2 + SrF_2, O_2, Pt \quad [2]$$

in the temperature range 1180 to 1360 K. In a strict sense, the reference electrode containing pure SrO is not stable in contact with CaF_2, which was used as the solid electrolyte. From a thermodynamic point of view, the displacement reaction

$$SrO\,(rs) + CaF_2\,(f) \rightarrow CaO\,(rs) + SrF_2\,(f) \quad [3]$$

$$\Delta G_3^\circ = -34{,}135 + 5.97T\ (\pm 4000)\ J\ mol^{-1} \quad [4]$$

can disturb the equilibrium at the reference-electrode/electrolyte interface. The rock-salt structure is represented by (rs) and the fluorite structure by (f). The free-energy data are taken from the compilations of Pankratz.[13,14] The equilibrium chemical potential of fluorine at the electrode/electrolyte interface may not be determined by the equilibrium between SrO, SrF_2, and O_2 as intended by the investigator. The actual fluorine chemical potential is likely to be displaced toward the value corresponding to the equilibrium between CaO, CaF_2, and O_2.

The standard free energy of formation of $BaZrO_3$ was measured by Levitskii[12] and Levitskii *et al.*[15] using the cell

$$Pt, O_2, CaO + CaF_2|CaF_2|BaZrO_3 + ZrO_2 + BaF_2, O_2, Pt \quad [5]$$

From the Gibbs energy change corresponding to the virtual cell reaction

$$BaF_2\,(f) + ZrO_2\,(m) + CaO\,(rs) \rightarrow BaZrO_3\,(c) + CaF_2\,(f) \quad [6]$$

the free energy of formation of cubic (c) $BaZrO_3$ was calculated, using auxiliary data from the literature for the other phases. However, combined uncertainties in the auxiliary data enhance the error limits on the derived properties of $BaZrO_3$.

To overcome the drawbacks in the design of cells used earlier,[12,15] new galvanic cells using single-crystal SrF_2 and BaF_2 as solid electrolytes were employed in this study to directly measure the Gibbs free energies of formation of $SrZrO_3$ and $BaZrO_3$ in the temperature range 960 to 1210 K:

$$Pt, O_2, SrO + SrF_2|SrF_2|SrF_2 + SrZrO_3 + ZrO_2, O_2, Pt \quad [7]$$

$$Pt, O_2, BaO + BaF_2|BaF_2|BaF_2 + BaZrO_3 + ZrO_2, O_2, Pt \quad [8]$$

The cells are written such that the right-hand electrodes are positive. An additional factor to be considered when using BaO as a reference electrode in cell [8] is the solubility of BaO_2 in BaO. The oxygen partial pressure in the gas phase over the electrodes has to be maintained at a sufficiently low value to minimize the solubility of BaO_2.[16] At the same time, the gas phase must have a reasonably high thermodynamic capacity for oxygen,[17] $C_{O_2} = (\partial n_{O_2}/\partial \mu_{O_2})_{T,P}$, to impose identical oxygen chemical potentials on both electrodes. The lower limit of oxygen partial pressure at which the fluoride cells operate satisfactorily was established empirically using cell [7]. Since SrO_2 is relatively less stable than BaO_2, it does not have significant solubility in SrO at atmospheric pressure of oxygen in the temperature range of measurement. It is also important to remove traces of CO_2 and H_2O from the gas phase, since they react readily with the reference materials SrO and BaO.

II. EXPERIMENTAL ASPECTS

A. *Materials*

The compounds $SrZrO_3$ and $BaZrO_3$ were prepared by heating mixtures of $SrCO_3$ + ZrO_2 in platinum crucibles at 1673 K for 160 ks under prepurified oxygen gas flowing at a rate of 5 mL s^{-1}. The high-purity oxygen gas was passed through sodium hydroxide to remove traces of CO_2 and then dried by passing through columns containing anhydrous magnesium perchlorate and phosphorus pentoxide. The carbonates and zirconia used for synthesis were of purity higher than 99.99 pct and were dried at 523 K before use. Stoichiometric amounts of the carbonate and zirconia were thoroughly mixed and pressed into pellets before heating first at 1200 K for 20 ks and then slowly to 1673 K. After firing for 80 ks, the pellets were cooled, reground to −270 mesh, and repelletized for further heat treatment. Completion of the reactions was confirmed by X-ray diffraction analysis of the products. At room temperature, $SrZrO_3$ was found to have the orthorhombic perovskite structure (*Pbnm*: D_{2h}^{16}; Z = 4) with a = 0.57964, b = 0.58170, and c = 0.82049 nm, rather than the cubic structure with a = 0.8208 nm (Z = 8) reported recently by Mathews *et al.*[18]

Gas mixtures containing argon and oxygen were made by mixing metered streams of each gas. The flow rates were set by mass-flow controllers. Two compositions, which were used extensively, were prepared by premixing the component gases in a cylinder. The oxygen partial pressure of each mixture, after removal of residual carbon dioxide and moisture, was determined using an oxygen meter based on yttria-stabilized zirconia as the solid electrolyte. Transparent single crystals of SrF_2

and BaF_2 for use as solid electrolytes were obtained in the form of disks 1.5 cm in diameter and 0.3-cm thick.

B. *Apparatus and Procedure*

The apparatus used in this study for electromotive force (emf) measurements was similar to that described earlier.[19,20] The electrode pellets were spring loaded on either side of the transparent single-crystal AF_2 (A = Sr, Ba), with a platinum gauze sandwiched between each electrode pellet and the electrolyte. Platinum electrical leads were spot-welded to the gauze. The pellets were held together under pressure by a system of alumina tubes and rods.[19,20] After assembling the cell and raising its temperature to 573 K, the outer alumina tube enclosing the cell was evacuated and then refilled with oxygen gas. The procedure was repeated three times to remove moisture adsorbed on ceramic tubes. The cells were then operated under flowing mixtures of argon and oxygen. The same gas mixture flowed over both electrodes. The reversible emfs of cells [7] and [8] were measured as a function of temperature. The emf of cell [7] was also monitored as a function of the partial pressure of oxygen in the gas phase. The emf was found to be reproducible and independent of oxygen partial pressures greater than 10 Pa. The emf response became markedly sluggish below an oxygen partial pressure of 10 Pa in the gas phase. The emf of cell [8] was measured using a gas phase with an oxygen partial pressure of 18.7 Pa. The emfs of the cells were independent (±1 mV) of the flow rate of the gas in the range 1.5 to 5 mL s^{-1}. Most of the measurements were made at a constant flow rate of 2.5 mL s^{-1}. The temperature of the cell was measured with a Pt/Pt-13 pct Rh thermocouple.

The emfs became steady in 7 to 30 ks after the attainment of thermal equilibrium, depending on the temperature of the cells. The reversibility of the cells was checked by microcoulometric titration in both directions. In each case, the cell emf returned to its original value before titration within 2 ks. This demonstrated that the chemical potential of fluorine at the electrodes returned to the same value after essentially infinitesimal displacements from equilibrium to lower and higher values. The emfs were reproducible on repeated temperature cycling. At the end of each experiment, the cell was cooled, and the electrodes were examined by X-ray diffraction. No changes in the phase composition of the electrodes during the emf measurement could be detected. Since the emf of cell [7] exhibited a change in slope as a function of temperature at 1123 K, lattice parameters of $SrZrO_3$ and $BaZrO_3$ were measured as a function of temperature using Cu K_α radiation to check for phase transitions. A thin layer of $SrZrO_3$ powder was mounted on a platinum strip heater. A recent X-ray diffraction study of $SrZrO_3$[18] from 298 to 1675 K in air has not detected any phase transition; the structure is reported to be cubic in the entire temperature range.

The most important factor for successful operation of the emf cells used in this study was the removal of trace amounts of CO_2 and H_2O from the gas phase. Reaction of the fluoride electrolytes with moisture results in an opaque coating of the corresponding oxides on their surface. The reference electrodes also react readily with CO_2 and H_2O in the gas phase, leading to unsteady emfs.

III. RESULTS AND DISCUSSION

A. *Emf Measurements*

The reversible emfs of cells [7] and [8] are shown as a function of temperature in Figures 1 and 2, respectively. The numbers and letters on the figures indicate the sequence of measurements. The emf of cell [7] is independent of the partial pressure of oxygen in the gas phase. The emf plot for this cell appears to change its slope at approximately 1123 K. It is difficult to determine the exact transition temperature from the emf results. The emf for cell [7] was therefore fitted using two linear equations, one below and the other above 1123 K. The least-squares regression analysis gives

$$E_7' = 388.0 + 7.36 \times 10^{-2}T\ (\pm 0.7)\ \text{mV} \qquad [9]$$

for $T \leq 1123$ K. At higher temperatures,

$$E_7'' = 381.6 + 7.93 \times 10^{-2}T\ (\pm 0.9)\ \text{mV} \qquad [10]$$

The uncertainty limits correspond to twice the standard error estimate. Since neither SrO nor ZrO_2 has a phase transition at 1123 K, the change in slope of the emf suggests a phase transition in $SrZrO_3$. This was confirmed by X-ray studies described in the Section IV.

The electrochemical reaction at the right electrode of cell [7] is

$$SrF_2\ (f) + 2e^- + 0.5O_2\ (g) + ZrO_2\ (m) \rightarrow SrZrO_3\ (o, t) + 2F^- \qquad [11]$$

where (m) denotes monoclinic, (o) orthorhombic, and (t) tetragonal structures, and (g) indicates gas phase.

The corresponding reaction at the left electrode is

$$2F^- + SrO\ (rs) \rightarrow SrF_2\ (f) + 0.5\ O_2\ (g) + 2e^- \qquad [12]$$

The virtual cell reaction corresponding to cell [7], obtained by combining the electrochemical reactions at the two electrodes, is

$$SrO\ (rs) + ZrO_2\ (m) \rightarrow SrZrO_3\ (o) \qquad [13]$$

in the temperature range 960 to 1123 K and

$$SrO\ (rs) + ZrO_2\ (m) \rightarrow SrZrO_3\ (t) \qquad [14]$$

from 1123 to 1210 K. The transport number of fluoride ions is greater than 0.99 in SrF_2 and BaF_2 in the range of temperatures and fluorine chemical potentials covered in this study. Therefore, the standard free-energy change corresponding to these reactions can be computed directly from the emf using the Nernst equation:

$$\Delta G_{13}^\circ = -2FE_7' = -74{,}880 - 14.2T\ (\pm 200)\ \text{J mol}^{-1} \qquad [15]$$

$$\Delta G_{14}^\circ = -2FE_7'' = -73{,}645 - 15.3T\ (\pm 200)\ \text{J mol}^{-1} \qquad [16]$$

The transformation of $SrZrO_3$ from orthorhombic to tetragonal perovskite structure at 1123 (±10) K is associated with an enthalpy change of 1235 (±600) J mol^{-1} and entropy change of 1.10 (±0.53) J K^{-1} mol^{-1}. It would be interesting to confirm these values by calorimetry.

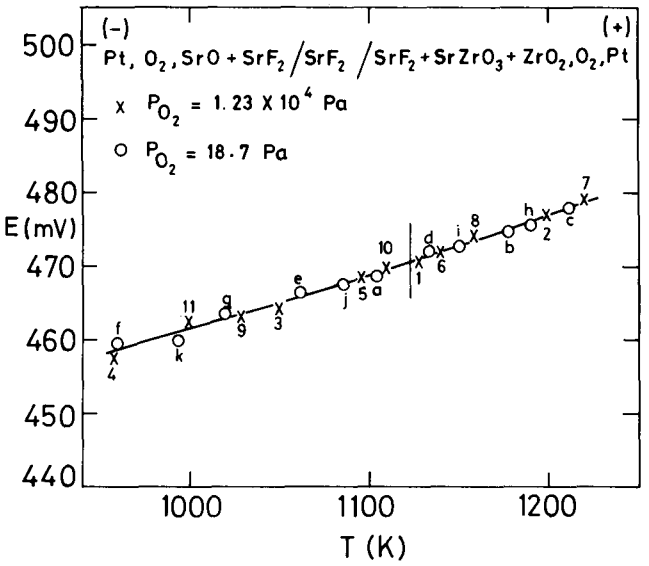

Fig. 1—The temperature dependence of the reversible emf of cell [7] at two different partial pressures of oxygen. The numbers and letters indicate the sequence of measurement.

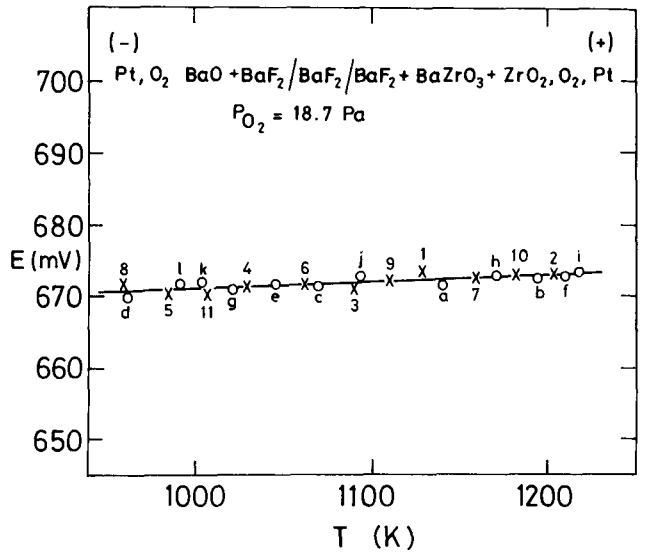

Fig. 2—The variations of the reversible emf of cell [8] with temperature.

Values for the free energy of formation of $SrZrO_3$ obtained in this study are compared with those reported by Levitskii[12] in Table I. The extrapolated values are in parentheses. At a temperature of 1200 K, common to both investigations, the standard free energy of formation of $SrZrO_3$ from component oxides obtained in the present study is 6.1 kJ mol^{-1} more negative than that given by Levitskii.[12] As discussed in Section I, particles of SrO in contact with CaF_2 at the reference-electrode-/electrolyte interface of the cell used by Levitskii[12] would have reacted slowly to form CaO and SrF_2. The fluorine chemical potential corresponding to the equilibrium CaO + CaF_2 + O_2 is more positive by 27.0 kJ mol^{-1} at 1200 K than that corresponding to the equilibrium SrO + SrF_2 + O_2, when oxygen potentials are identical.[13,14] Because of the occurrence of the solid-state displacement reaction [3] at a relatively slow rate at the electrode/electrolyte interface, a mixed potential lying between the two equilibrium states would have prevailed. Consequently, the emf would be lower and the derived free energy of formation less negative. With increasing temperature, the rate of the displacement reaction and the deviation of the fluorine chemical potential at the electrode/electrolyte interface from the equilibrium value corresponding to the SrO + SrF_2 + O_2 electrode would be expected to increase. The values summarized in Table I support this interpretation.

Table I. Comparison of the Standard Free Energies of Formation of $SrZrO_3$ from Component Oxides

	ΔG° (kJ mol^{-1})	
T (K)	This Study	Levitskii[12]
1000	−89.08	(−85.19)
1100	−90.50	(−85.55)
1200	−92.01	−85.91
1300	(−93.54)	−86.27

The "second-law" enthalpy of formation of orthorhombic $SrZrO_3$ from component oxides in the temperature range 960 to 1123 K is −74.9 (±3) kJ mol^{-1}. This is in good agreement with the value of −75.9 (±4.5) kJ mol^{-1} at 1060 K obtained by Muromachi and Navrotsky[11] by high-temperature solution calorimetry. The second-law enthalpy of formation from oxides at 298.15 K is −77.9 (±2) kJ mol^{-1}. The "third-law" analysis of the free energy of formation of $SrZrO_3$ from component oxides obtained in this study gives $\Delta H^\circ_{f,\text{oxides}}$ = −76.4 (±0.2) kJ mol^{-1} at 298.15 K. The Gibbs energy functions for $SrZrO_3$ used in the analysis were taken from Nagarajan *et al.*,[7] those for ZrO_2 and SrO from Pankratz.[13] The close correspondence between the second-law and third-law enthalpies of formation at 298.15 K and the small drift with temperature of the third-law value indicate the lack of significant temperature-dependent errors in emf measurement. Using values for the standard enthalpies of formation of ZrO_2 (−1100.6 kJ mol^{-1}) and SrO (−560.5 kJ mol^{-1}) at 298.15 K from the compilation of Pankratz,[13] the standard enthalpy of formation of $SrZrO_3$ is obtained as ΔH°_f (298.15 K) = −1767.5 (±3) kJ mol^{-1}, in excellent agreement with the value of −1767.7 (±2) kJ mol^{-1} obtained by bomb calorimetry.[10]

The emf of cell [8] can be expressed by the linear relation

$$E_8 = 662.0 + 9.28 \times 10^{-3} T\ (\pm 0.9)\ \text{mV} \qquad [17]$$

in the temperature range 960 to 1210 K. There appears to be no phase transition in $BaZrO_3$ in this range. The standard free energy of formation of $BaZrO_3$ from component oxides, obtained from the emf, is

$$\text{BaO (rs)} + \text{ZrO}_2\text{ (m)} \rightarrow \text{BaZrO}_3\text{ (c)} \qquad [18]$$

$$\Delta G^\circ_{18} = -127{,}760 - 1.79T\ (\pm 250)\ \text{J mol}^{-1} \qquad [19]$$

The values obtained in this study at different temperatures are compared with the data reported by Levitskii[12] and Levitskii *et al.*[15] in Table II. The values suggested

Table II. Comparison of the Standard Gibbs Energies of Formation of $BaZrO_3$ from Component Oxides

	ΔG° (kJ mol^{-1})		
T (K)	This Study	Levitskii[12]	Levitskii (Recalculated)
1000	−129.55	(−136.40)	(−135.98)
1100	−129.73	(−136.61)	(−133.58)
1200	−129.91	−136.82	−131.30
1300	(−130.09)	−137.03	−129.29
	(±0.25)	(±4)	(±3)

by Levitskii and co-workers are considerably more negative; at 1200 K, the difference is 6.9 kJ mol^{-1}. The emf measurements of Levitskii and co-workers give the standard free-energy change for the reaction

$$BaF_2\,(f) + ZrO_2\,(m) + CaO\,(rs) \rightarrow BaZrO_3\,(c) + CaF_2\,(f) \quad [20]$$

The free energy of formation of $BaZrO_3$ from component oxides was obtained by combining the result with the standard free-energy change for the reaction

$$CaF_2\,(f) + BaO\,(rs) \rightarrow BaF_2\,(f) + CaO\,(rs) \quad [21]$$

from the literature. If more recent values for the free-energy change for reaction [21][13,14] are combined with the emf results of Levitskii[12] and Levitskii *et al.*[15] then the free energy of formation of $BaZrO_3$ is significantly altered. At a temperature of 1200 K, common to both this study and that of Levitskii and co-workers, the recalculated free energy of formation of $BaZrO_3$ from component oxides is more positive by 5.5 kJ mol^{-1}. The agreement between the results obtained by this study and the recalculated value at 1200 K is good, although the temperature coefficient of the free energy differs significantly.

The second-law enthalpy of formation of $BaZrO_3$ from component oxides obtained in this study [−127.76 (±2) kJ mol^{-1} at 1085 K] is in reasonable agreement with the value of −123.9 (±4.1) kJ mol^{-1} obtained by Muromachi and Navrotsky[11] at 1060 K using high-temperature solution calorimetry. The second-law enthalpy of formation at 298.15 K from the results of this study is −125.56 (±2) kJ mol^{-1}. The third-law analysis gives a value of −126.64 (±0.14) kJ mol^{-1} at 298.15 K, with a very small drift (0.25 kJ mol^{-1}) with temperature. The Gibbs energy functions for $BaZrO_3$ used in the analysis were taken from Cordfunke and Konings,[9] those for BaO and ZrO_2 from Pankratz.[13] There is good agreement between the second-law and third-law values, confirming the reliability of emf measurements. The enthalpy of formation of $BaZrO_3$ from elements at 298.15 K, obtained by combining the result from the third-law analysis with the data in the literature for BaO and ZrO_2, is −1775.4 (±3) kJ mol^{-1}. Bomb calorimetric measurements of L'vova and Fedoslev[10] suggest a value of −1779.2 (±2) kJ mol^{-1}, in fair agreement with the value obtained in this study.

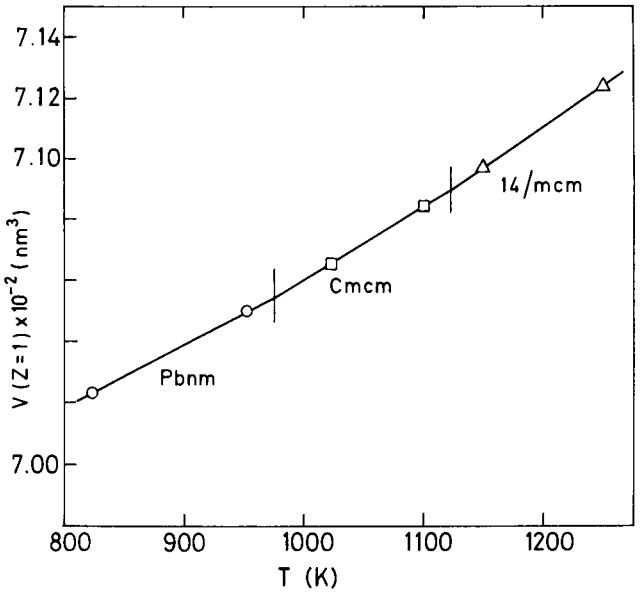

Fig. 3 — The variation of the unit cell volume (Z = 1) of $SrZrO_3$ with temperature.

B. *High-Temperature X-Ray Diffraction*

The powder X-ray patterns for $SrZrO_3$ and $BaZrO_3$ were analyzed using the Rietveld full pattern refinement technique. The Rietveld method, in principle, permits the refinement of unit cell dimensions and atomic positions in the crystal structure simultaneously. The fitting of the

Table III. Space Group and Lattice Dimensions of $SrZrO_3$ with Pervoskite Structure at Different Temperatures

Space Group	T (K)	a (nm)	b (nm)	c (nm)	V (nm^3)
Orthorhombic	295	0.57964	0.58170	0.82049	0.27665
(*Pbnm*)	423	0.58054	0.58225	0.82152	0.27769
D_{2h}^{16}	623	0.58195	0.58307	0.82311	0.27930
(Z = 4)	823	0.58336	0.58393	0.82472	0.28093
	953	0.58427	0.58448	0.82577	0.28200
Orthorhombic (*Cmcm*)	1023	0.82592	0.82764	0.82693	0.56526
D_{2h}^{17}	1100	0.82649	0.82865	0.82755	0.56677
(Z = 8)					
Tetragonal (14/*mcm*)	1150	0.58503	—	0.82949	0.28390
D_{4h}^{18}	1250	0.58587	—	0.83020	0.28496
(Z = 4)					

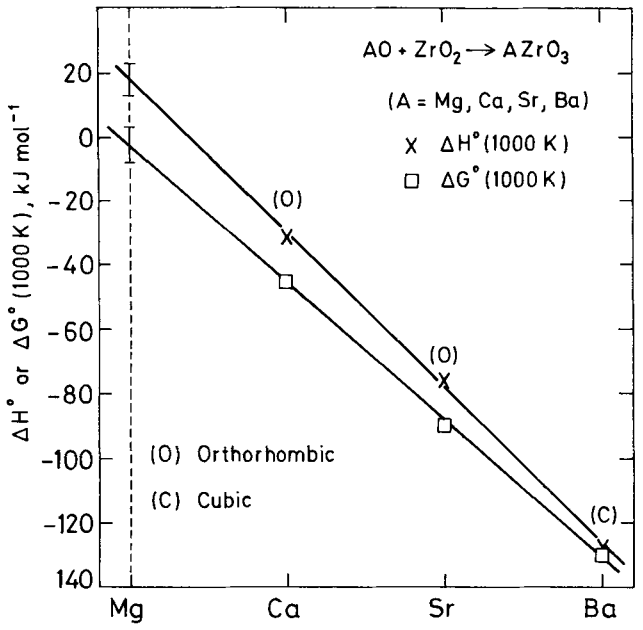

Fig. 4—Systematic trends in the high-temperature enthalpy and Gibbs energy of formation of $AZrO_3$ (A = alkaline-earth element) compounds.

Table IV. Unit Cell Dimensions of $BaZrO_3$ at Different Temperatures

Structure/ Space Group	T (K)	a (nm)	V (nm^3)
Cubic perovskite	295	0.41897	0.073544
	423	0.41934	0.073739
$Pm\bar{3}m$	623	0.41993	0.074051
O_h^1	823	0.42054	0.074374
(Z = 1)	1023	0.42114	0.074693
	1123	0.42145	0.074858

diffraction profile is achieved by a least-squares method of minimizing the differences between measured and calculated patterns. The X-ray scattering from $SrZrO_3$ and $BaZrO_3$ was dominated by contributions from the heavy atoms; oxygen atoms made only a relatively small contribution. Therefore, it was difficult to refine the oxygen positions using X-ray data alone. Fortunately, high-temperature neutron powder diffraction studies have been reported by Ahtee and co-workers[21,22] for $SrZrO_3$. The oxygen positions from neutron studies were used initially for structure analysis. Later, the refinements were conducted by releasing all the atomic positions. The resulting lattice parameters did not differ significantly from those obtained using oxygen positions from neutron studies. The R factor representing the difference between the experimental and calculated profiles varied from 0.007 to 0.008.

The lattice parameters of $SrZrO_3$ obtained at different temperatures are summarized in Table III. The unit cell volumes for the different phases, reduced to pseudocubic cell (Z = 1), are shown as a function of temperature in Figure 3. The room-temperature orthorhombic perovskite structure having the space group $Pbnm$: D_{2h}^{16} was found to change to another orthorhombic phase with space group $Cmcm$: D_{2h}^{17} at approximately 975 K. The next structure transition to tetragonal perovskite with space group $14/mcm$: D_{4h}^{18} occurs at around 1123 K. The transition temperatures obtained from the changes in slope of unit cell volume in Figure 3 are only correct to ±10 K. The X-ray studies confirm the phase transition in $SrZrO_3$ detected during emf measurements. The results of the study are in total disagreement with the findings of Mathews *et al.*,[18] who determined the structure of $SrZrO_3$ as cubic in the temperature range 298 to 1675 K.

The lattice dimensions for $BaZrO_3$ are summarized in Table IV. The structure is cubic with space group $Pm\bar{3}m$: O_h^1 from room temperature to 1250 K. The molar volumes of the zirconates can be readily calculated as a function of temperature from the unit cell volumes listed in Tables III and IV. Information on molar volume permits the estimation of the stability of the zirconates as a function of pressure. The variation in unit cell dimensions of each structural phase of $SrZrO_3$ and $BaZrO_3$ can be fitted reasonably well with linear equations. The linear and volume thermal expansion coefficients for all the phases studied are presented in Table V. There is significant anisotropy in linear thermal expansion for all phases except cubic.

C. *Stability of Alkaline-Earth Zirconates—Trends*

It is useful to compare the stabilities of the alkaline-earth zirconates with perovskite structure. The standard free energy and enthalpy of formation of the zirconates with $AZrO_3$ stoichiometry at 1000 K are shown as a function of the periodicity of the alkaline-earth element in Figure 4. Surprisingly, both the enthalpy and free energy of formation of calcium,[2] strontium, and barium zirconates obtained by the emf technique can be approximated by linear relations. Extrapolation indicates a

Table V. Thermal Expansion Coefficients (α) for $SrZrO_3$ and $BaZrO_3$ ($\times 10^5$) K^{-1}

Compound/ Space Group	Temperature Range (K)	α_a	α_b	α_c	α_V
$SrZrO_3$					
Orthorhombic (*Pbnm*)	295 to 953	1.209	0.725	0.975	2.909
Orthorhombic (*Cmcm*)	1023 to 1100	0.896	1.584	0.934	3.458
Tetragonal (14/*mcm*)	1150 to 1250	1.435	—	0.856	3.723
$BaZrO_3$					
Cubic ($Pm\bar{3}m$)	295 to 1150	0.713	—	—	2.139

positive enthalpy of formation [18 (±5) kJ mol^{-1}] of $MgZrO_3$ from its component oxides. The free energy is marginally negative, but given the uncertainties in the data and extrapolation, no definite conclusions can be drawn. The compound $MgZrO_3$ has not been synthesized. Even if the compound is unstable in the binary MgO-ZrO_2 system, it may be stabilized by solid solution formation in ternary and higher order systems. Extensive solid solutions with other structurally compatible perovskites may be expected.

IV. SUMMARY

The standard Gibbs free energies of formation of the high-temperature orthorhombic and tetragonal forms of $SrZrO_3$ and cubic perovskite $BaZrO_3$ have been determined in the temperature range 960 to 1210 K using potentiometric measurements on solid-state cells employing single crystals of SrF_2 and BaF_2, respectively, as solid electrolytes. From the change in the slope of emf as a function of temperature, a phase transition from orthorhombic to tetragonal perovskite structure has been identified in $SrZrO_3$ at 1123 (±10) K. High-temperature X-ray diffraction studies have confirmed the transition. The linear and volume thermal expansion coefficients of $SrZrO_3$ and $BaZrO_3$ have been derived from high-temperature structural measurements. The thermodynamic data obtained in this study are in good agreement with bomb and high-temperature solution calorimetric measurements on enthalpies of formation of the zirconates. They are also consistent with calorimetric entropies reported in the literature. A review of the systematic trends in the stability of alkaline-earth zirconates having the stoichiometry $AZrO_3$ indicates that magnesium zirconate would be unstable relative to its component binary oxides at low temperatures.

REFERENCES

1. D. Janke: *Metall. Trans. B*, 1982, vol. 13B, pp. 227-35.
2. K.T. Jacob and Y. Waseda: *Thermochim. Acta*, 1994, vol. 239, pp. 233-41.
3. E.H.P. Cordfunke and R.J.M. Konings: *J. Nucl. Mater.*, 1988, vol. 152, pp. 301-09.
4. E.H.P. Cordfunke and R.J.M. Konings: *Thermochemical Data for Reactor Materials and Fission Products*, North-Holland, Amsterdam, 1990.
5. E.G. King and W.W. Weller: U.S. Bureau of Mines Rep. Invest. 5571, Department of the Interior, Washington, DC, 1960.
6. V.A. Levitskii, D.Sh. Tsagareishvili, and G.G. Gvelesiani: *Teplofiz. Vys. Temp.*, 1976, vol. 14, pp. 78-84.
7. K. Nagarajan, R. Saha, R. Babu, and C.K. Mathews: *Thermochim. Acta*, 1985, vol. 90, pp. 297-304.
8. E.N. Fomichev, N.P. Slyusar, A.D. Krivorotenko, and V.Ya. Tolstaya: *Ogneupory*, 1973, vol. 7, pp. 36-39.
9. E.H.P. Cordfunke and R.J.M. Konings: *Thermochim. Acta*, 1989, vol. 156, pp. 45-51.
10. A.S. L'vova and N.N. Fedos'ev: *Russ. J. Phys. Chem.*, 1964, vol. 38, p. 14.
11. E.T. Muromachi and A. Navrotsky: *J. Solid State Chem.*, 1988, vol. 72, pp. 244-56.
12. V.A. Levitskii: *J. Solid State Chem.*, 1978, vol. 25, pp. 9-22.
13. L.B. Pankratz: *Thermodynamic Properties of Elements and Oxides*, U.S. Bureau of Mines Bull. 672, Department of the Interior, Washington, DC, 1982.
14. L.B. Pankratz: *Thermodynamic Properties of Halides*, U.S. Bureau of Mines Bull. 674, Department of the Interior, Washington, DC, 1984.
15. V.A. Levitskii, Yu. Ya. Skolis, Yu. Kheminov, and N.N. Shevchenko: *Russ. J. Phys. Chem.*, 1974, vol. 48, pp. 24-27.
16. O.V. Kedrovskii, I.V. Kovtunenko, E.V. Kiseleva, and A.A. Bundel: *Russ. J. Phys. Chem.*, 1967, vol. 41, pp. 205-08.
17. R. Akila, K.T. Jacob, and A.K. Shukla: *Bull. Mater. Sci.*, 1986, vol. 8, pp. 453-65.
18. M.D. Mathews, E.B. Mirza, and A.C. Momin: *J. Mater. Sci. Lett.*, 1991, vol. 10, pp. 305-06.
19. K.T. Jacob and J.P. Hajra: *Bull. Mater. Sci.*, 1987, vol. 9, pp. 37-46.
20. K.T. Jacob, K.P. Abraham, and S. Ramachandran: *Metall. Trans. B*, 1990, vol. 21B, pp. 521-27.
21. A. Ahtee, M. Ahtee, A.M. Glazer, and A.W. Hewat: *Acta Crystallogr.*, 1978, vol. B32, pp. 3243-46.
22. M. Ahtee, A.M. Glazer, and A.W. Hewat: *Acta Crystallogr.*, 1978, vol. B34, pp. 752-58.